Defect Stream Function, Law of the Wall/Wake Method for Compressible Turbulent Boundary Layers

Richard A. Wahls*
North Carolina State University, Raleigh, North Carolina 27695
Richard W. Barnwell†
NASA Langley Research Center, Hampton, Virginia 23665
and
Fred R. DeJarnette‡
North Carolina State University, Raleigh, North Carolina 27695

The application of the defect stream function to the solution of the two-dimensional, compressible boundary layer is examined. A law-of-the-wall/law-of-the-wake formulation for the inner part of the boundary layer is presented which greatly simplifies the computational task near the wall and eliminates the need for an eddy viscosity model in this region. The eddy viscosity model in the outer region is arbitrary. The modified Crocco temperature-velocity relationship is used in lieu of the energy equation. Formulations for both equilibrium and nonequilibrium boundary layers are presented including a constrained zero-order form which significantly reduces the computational workload while retaining the significant physics of the flow. Results are given for the constrained zero-order and second-order equilibrium formulations and are compared with experimental data. A compressible wake function valid near the wall has been developed from the present results.

Introduction

TURBULENT flow analyses are all based on empiricism to some extent. The law of the wall, with the law of the wake as a corollary, is one of the most well-established, widely accepted, and accurate empiricisms in fluid mechanics.[1] The general purpose of the present research is to exploit the law of the wall and law of the wake in order to improve both the accuracy and efficiency of computational fluid dynamics. These laws are used to model the flow in the inner part of turbulent boundary layers; the outer or defect part of the boundary layer is solved computationally.

The present authors began this effort by developing a procedure for incompressible flow. The first method[2] combined an integral treatment of the inner layer with a finite-difference treatment of the outer layer. The problem was formulated in terms of the conventional stream function, and solutions were obtained for incompressible flow over a flat plate, a two-dimensional circular cylinder, and two-dimensional elliptic cylinders. Although successful computations were made in which pressure gradient effects were accounted for, a fair amount of numerical difficulty was encountered.

A second incompressible method[3] was developed which reduced the numerical difficulty by replacing, where possible, computational steps in the interaction algorithm with equivalent analytical steps. This method was formulated in terms of the defect stream function used by Mellor and Gibson[4] and validated experimentally by Clauser.[5] The defect stream function was chosen because it properly characterizes the flow in the outer region of the boundary layer, which must be solved numerically, and because it has the remarkable property of having a first integral, to lowest order in the nondimensional shear stress velocity ratio, in the direction normal to the surface. This property facilitates the implementation of the integral treatment in the inner region.

Two major problems with the defect stream-function formulation encountered in Ref. 4 concerned the enforcement of law-of-the-wall behavior near the wall and the implementation of the wall-layer eddy viscosity model. The computational complexity Mellor and Gibson encountered in the inner region probably explains the general lack of popularity of the defect stream-function formulation. The incompressible method of Ref. 3 completely overcomes this complexity. Accuracy in the inner region is an additional advantage of the method of Ref. 3 over that of Ref. 4; it was shown that the results of the latter agree with the law of the wall only very near the wall whereas the results of the former are correct across the inner layer.

The present compressible method is an extension of the method of Ref. 3. The van Driest effective velocity approach[6] is used as the law of the wall, and the Crocco temperature-velocity relationship modified with a recovery factor is used as an approximation of the energy equation. This initial compressible flow effort is limited to adiabatic wall flows. The coordinate transformation incorporates a density weighting integral in the normal direction similar to that used by Mager,[7] among others.

The present law-of-the-wake treatment differs considerably from that of Ref. 3, where the incompressible correlation of White[8] was used. It is shown that the wake function, which is used only in the inner region and at the boundary with the outer region, can be evaluated with the difference between the outer numerical solution and the law of the wall at several points just beyond the inner region. It is found that results for incompressible flow confirm White's correlation and that compressibility effects can be correlated with a single additional parameter.

Received Jan. 25, 1989; revision received Feb. 27, 1989.

*Graduate Research Assistant; presently Research Engineer, Vigyan, Hampton, VA. Student Member AIAA.
†Chief Scientist. Associate Fellow AIAA.
‡Professor of Mechanical and Aerospace Engineering. Associate Fellow AIAA.

There are several other current methods which use a law-of-the-wall formulation in the inner region. Wall-function methods such as that of Viegas et al.[9] simply patch the numerical and analytic solutions at the first grid point and employ an eddy viscosity model throughout the boundary layer. The recent method of Walker et al.[10] is similar to the present approach in that it interacts inner-layer (viscous sublayer) analytic solutions with outer numerical solutions at a point determined in the analysis. The Walker method uses the conventional stream-function formulation and both an inner and outer eddy viscosity model. Wilcox[11] employs the defect stream-function formulation but uses an eddy viscosity across the entire boundary layer; he does not make use of the first integral property of the defect stream-function formulation.

Defect Stream-Function Formulation

The basic formulation is an extension of the incompressible method of Ref. 3. The treatment is for nonequilibrium boundary layers, and the eddy viscosity model is arbitrary. In fact, it is unnecessary to specify the eddy viscosity in the inner layer at all.

Basic Equations

The continuity and momentum equations for compressible turbulent boundary-layer flow are

$$\frac{\partial \rho u}{\partial x}+\frac{\partial \rho v}{\partial y}=0 \tag{1}$$

$$\rho u\frac{\partial u}{\partial x}+\rho v\frac{\partial u}{\partial y}-\rho_e u_e\frac{\mathrm{d}u_e}{\mathrm{d}x}=\frac{\partial}{\partial y}\left[(\mu+\mu_t)\frac{\partial u}{\partial y}\right] \tag{2}$$

where x and y are the tangential and normal coordinates, u and v are the respective velocity components, ρ is the density, μ is the viscosity, and ρ_e and u_e are the edge density and edge velocity. The sum of μ and the eddy visosity μ_t is

$$\mu+\mu_t=K(x,y)\rho u_e\delta_i^* \tag{3}$$

where K is a general nondimensional function of x and y and δ_i^* is the incompressible displacement thickness. The energy equation is approximated with the modified Crocco temperature-velocity relationship. For adiabatic walls, this relationship is

$$\frac{T_w}{T}=\frac{\rho}{\rho_w}=1+r\frac{(\bar\gamma-1)}{2}\left(\frac{u}{a}\right)^2=1+r\frac{(\bar\gamma-1)}{2}M^2 \tag{4}$$

where $\bar\gamma$ is the ratio of specific heats (taken to be 1.4), a is the speed of sound, M is the Mach number, the subscript w denotes values at the wall, and $r=Pr^{1/3}$ is the recovery factor for turbulent flow where Pr is the Prandtl number. The Prandtl number is assumed to be 0.72 in the present study.

In this treatment, the defect stream function of Clauser,[5] as used in Ref. 3, is modified to account for compressibility. This function is defined as

$$f'(\xi,\eta)=\frac{\partial f}{\partial \eta}=\frac{u-u_e}{u^*} \tag{5}$$

where

$$\xi=x,\ \eta=\frac{1}{\Delta}\int_0^y\frac{\rho}{\rho_e}\,\mathrm{d}y \tag{6}$$

The shear stress velocity u^* is defined as

$$u^*=(\tau_w/\rho_w)^{1/2}$$

where ρ_w and τ_w are the density and shear stress at the wall.

The boundary-layer thickness parameter Δ is defined as

$$\Delta=-\int_0^\infty\frac{\rho}{\rho_e}f'\,\mathrm{d}y=\frac{u_e}{u^*}\int_0^\infty\frac{\rho}{\rho_e}\left(1-\frac{u}{u_e}\right)\mathrm{d}y=\frac{u_e\delta_v^*}{u^*}$$

or

$$\Delta u^*=u_e\delta_v^* \tag{7}$$

where δ_v^* is a density-weighted velocity thickness. Partial derivatives with respect to x and y are of the form

$$\frac{\partial}{\partial x}=\frac{\partial}{\partial \xi}+\frac{\partial \eta}{\partial x}\frac{\partial}{\partial \eta};\qquad \frac{\partial}{\partial y}=\frac{\rho}{\Delta\rho_e}\frac{\partial}{\partial \eta} \tag{8}$$

Law of the Wall and Wake

It is assumed that a law of the wall and wake for the inner part of the boundary layer is known. This law is of the form

$$\frac{u}{u^*}=g(y^+,M_e)+h(\beta,\bar\eta,M_e) \tag{9}$$

where g is the law of the wall and h is the law of the wake. The inner variable y^+ is defined as

$$y^+=\frac{u^*y}{\nu_w}=\frac{Re_{\delta^*}}{\omega}\bar\eta \tag{10}$$

where ω and $\bar\eta$ are defined as

$$\omega=\frac{\delta_i^*}{\delta_v^*},\qquad \bar\eta=\frac{y}{\Delta}$$

and the Reynolds number based on the edge velocity, the incompressible displacement thickness, and the kinematic viscosity at the wall is defined as

$$Re_{\delta^*}=\frac{u_e\delta_i^*}{\nu_w}=\frac{u^*\Delta}{\nu_w}\omega$$

The compressible pressure-gradient parameter, which reduces to Clauser's pressure-gradient parameter for incompressible flow, is defined as

$$\beta=\frac{\delta_v^*}{\tau_w}\frac{\mathrm{d}p}{\mathrm{d}x} \tag{11}$$

A modified form of the parameter β will be defined later and shown to be the compressible equilibrium parameter. For nonequilibrium flow, this new parameter is a function of x and hence ξ; for equilibrium flow, this parameter is constant. In the present treatment, van Driest's effective velocity approach for adiabatic wall flows is used for the law of the wall where

$$g(y^+,M_e)=\frac{\sin\theta}{\chi\kappa} \tag{12a}$$

$$\chi=\frac{\gamma}{\kappa}\left(1-\frac{\rho_w}{\rho_e}\right)^{1/2},\qquad \theta=\chi\kappa\left(\frac{1}{\kappa}\ell n\,y^+ +B\right) \tag{12b}$$

and γ is the shear stress velocity ratio defined in the next section. The von Karman coefficients κ and B are given values of 0.41 and 4.9, respectively.

The leading term of the incompressible wake function is widely accepted to vary as y^2, but there is disagreement over the order of the higher-order terms. Although Moses and Coles agree on the leading term, the former uses a second term proportional to y^3, and the latter uses y^4.[6] Since the wake function is used only near the wall in the present

analysis, it is approximated with the one-term expansion

$$h(\beta,\bar{\eta},M_e) = \frac{6}{\kappa} w_1 \bar{\eta}^2 \tag{13}$$

The coefficient $w_1 = w_1(\beta,M_e)$ is determined with a least-squares curve fit of the difference between the outer-layer numerical solution and the law of the wall; this difference varies linearly with y^2 in the region just outside the inner layer. The value of w_1 is adjusted as part of the iterative solution. With this procedure, no additional empirical parameters are needed to enforce the law of the wake. In the Results and Discussion section, it is shown that the present results for wake-function compressibility effects can be correlated with a single additional parameter.

White[8] has correlated experimental data to determine the incompressible wake function. This correlation is

$$w_1 = \Pi\left(\frac{1+\Pi}{\kappa}\right)^2, \qquad \Pi = 0.8(0.5+\beta)^{0.75}$$

Shear Stress Velocity Ratio

The nondimensional shear stress velocity is defined as

$$\gamma = \frac{u^*}{u_e}$$

In the present treatment, the ratio γ is evaluated with the law of the wall/law of the wake. From Eqs. (5) and (9), it is seen that at the point η_m, which separates the inner and outer parts of the boundary layer, u can be expressed as

$$u = u^*[g(y_m^+) + h(\bar{\eta}_m)] = u_e + u^* f'(\xi,\eta_m)$$

The equation for γ is obtained from this equation as

$$\gamma = [g_m + h_m - f'_m]^{-1} \tag{14}$$

The gradient of γ is

$$\dot{\gamma} = -\gamma^2[\dot{g}_m + \dot{h}_m - \dot{f}'_m] \tag{15}$$

where the dot represents differentiation with respect to ξ. With Eqs. (10) and (12), the expression

$$\dot{g} = \frac{1}{\kappa}\left[\frac{\dot{\gamma}}{\gamma} + \frac{\dot{u}_e}{u_e} + \frac{\dot{\Delta}}{\Delta} - \frac{\dot{v}_w}{v_w}\right] + O\left[\left(\frac{u^*}{a_{aw}}\right)^2\right] \tag{16}$$

is obtained where

$$\frac{u^*}{a_{aw}} = \gamma M_e(\rho_w/\rho_e)^{1/2} \tag{17}$$

Substituting Eq. (16) into Eq. (15), one can write

$$\frac{u_e\dot{\gamma}}{\dot{u}_e\gamma} = \frac{-\left(\frac{\gamma}{\kappa}\right)}{\left(1+\frac{\gamma}{\kappa}\right)}\left[1 + \frac{u_e}{\dot{u}_e}\left(\frac{\dot{\Delta}}{\Delta} - \frac{\dot{v}_w}{v_w}\right)\right] + \frac{\rho_e}{\rho_w}\frac{\Delta}{\beta}\frac{(\dot{h}_m - \dot{f}'_m)}{\left(1+\frac{\gamma}{\kappa}\right)} \tag{18}$$

The analysis will also require the following expressions:

$$\frac{\dot{\rho}_e}{\rho_e} = -M_e^2\frac{\dot{u}_e}{u_e} \tag{19}$$

$$\frac{\dot{v}_w}{v_w} = \frac{\dot{\mu}_w}{\mu_w} - \frac{\dot{\rho}_w}{\rho_w} \tag{20}$$

with

$$\frac{\dot{\mu}_w}{\mu_w} = \left[\frac{1+3\frac{\bar{s}}{T_w}}{2\left(1+\frac{\bar{s}}{T_w}\right)}\right]\left[2\left(1-\frac{\rho_w}{\rho_e}\right)\frac{(r-1)}{r}\right]\frac{\dot{u}_e}{u_e}$$

$$\frac{\dot{\rho}_w}{\rho_w} = -\left[M_e^2 + 2\left(1-\frac{\rho_w}{\rho_e}\right)\left(1+\frac{\frac{\rho_e}{\rho_w}-1}{r}\right)\right]\frac{\dot{u}_e}{u_e}$$

where Sutherland's viscosity law is used and $\bar{s} = 199$ °R. Note that the term $u_e\dot{v}_w/\dot{u}_e v_w$ is a known function of M_e.

Governing Equations

Now one equation for the defect stream function f can be written. With Eqs. (5) and (8), the gradients of u and v, with respect to x and y, are found to be

$$\frac{\partial u}{\partial x} = \dot{u}_e(1+\gamma f') + u_e\frac{\partial}{\partial\xi}(\gamma f') + \frac{\partial\eta}{\partial x}u_e\gamma f''$$

$$\frac{\partial u}{\partial y} = \frac{\rho u_e \gamma f''}{\rho_e\Delta}$$

With Eq. (1), it can be shown that

$$-\rho v = (\eta+\gamma f)\frac{\mathrm{d}}{\mathrm{d}\xi}(\rho_e u_e\Delta) + \rho_e u_e\Delta\frac{\partial}{\partial\xi}(\gamma f) + \frac{\partial\eta}{\partial x}\rho_e u_e\Delta(1+\gamma f') \tag{21}$$

Let s be a nondimensional tangential coordinate of the form

$$s = \int^{\xi}\frac{\gamma}{\Delta}\,\mathrm{d}\xi$$

With this definition and Eq. (18), the tangential momentum equation can be written as

$$\frac{\omega}{\beta}\frac{\rho_e}{\rho_w}\left[K\left(\frac{\rho}{\rho_e}\right)^2 f''\right]' + \frac{\rho_e}{\rho_w}(2f' + \gamma f'^2) - \left(1+\frac{u_e\dot{\Delta}}{\dot{u}_e\Delta}\right)\left[(\eta+\gamma f)f'' + \frac{\left(\frac{\gamma}{\kappa}\right)}{\left(1+\frac{\gamma}{\kappa}\right)}\{f' + \gamma f'^2 - \gamma f f''\}\right]$$

$$+ M_e^2(\eta+\gamma f)f'' + \frac{\left(\frac{\gamma}{\kappa}\right)}{\left(1+\frac{\gamma}{\kappa}\right)}\frac{u_e\dot{v}_w}{\dot{u}_e v_w}(f' + \gamma f'^2 - \gamma f f'') + \frac{\left(\frac{\gamma}{\beta}\right)}{\left(1+\frac{\gamma}{\kappa}\right)}\frac{\rho_e}{\rho_w}\left(\frac{\mathrm{d}h_m}{\mathrm{d}s} - \frac{\mathrm{d}f'_m}{\mathrm{d}s}\right)(f' + \gamma f'^2 - \gamma f f'')$$

$$= \frac{\rho_e}{\rho_w}\frac{1}{\beta}\left(\frac{\partial f'}{\partial s} + \gamma f'\frac{\partial f'}{\partial s} - \gamma f''\frac{\partial f}{\partial s}\right) \tag{22}$$

Boundary Conditions

There are three boundary conditions for f. From Eq. (21) for ρv, the normal flow boundary condition at the surface, $v = 0$ at $\eta = 0$, is observed to correspond to

$$f = 0, \qquad \eta = 0$$

The value of f_∞ is obtained from the definition of the boundary-layer thickness Δ:

$$\Delta = -\int_0^\infty \frac{\rho}{\rho_e} f' \, dy = -\Delta \int_0^\infty f' \, d\eta = \Delta[f(0) - f_\infty]$$

$$f_\infty = -1 \tag{23}$$

The final boundary condition involves the shear stress at the wall. The condition is

$$\tau_w = \lim_{y \to 0} (\mu + \mu_t) \frac{\partial u}{\partial y}$$

This equation can be written as

$$\rho_w u^{*2} = \lim_{\eta \to 0} \frac{K(\xi,\eta)\rho^2 u_e^2 \delta_i^* \gamma f''}{\rho_e \Delta}$$

or

$$\lim_{\eta \to 0} K(\xi,\eta)\left(\frac{\rho}{\rho_e}\right)^2 f'' = \frac{1}{\omega}\frac{\rho_w}{\rho_e} \tag{24}$$

These boundary conditions reduce to those of Ref. 3 for incompressible flow.

First Integral of Governing Equation

With the boundary condition of Eq. (24), Eq. (22) can be integrated across the boundary layer to evaluate the quantity $1 + (\dot{\Delta} u_e / \Delta \dot{u}_e)$. The value is

$$\begin{aligned} 1 + \frac{\dot{\Delta} u_e}{\Delta \dot{u}_e} = &-\left[\left(1 + \frac{\gamma}{\kappa}\right)\left(\frac{1}{\beta} + \frac{\rho_e}{\rho_w}\{2 - \gamma G\} - M_e^2\{1 - \gamma G\}\right.\right. \\ &\left. - \frac{\gamma/\kappa}{(1+\gamma/\kappa)}\frac{u_e \dot{v}_w}{\dot{u}_e v_w}(2\gamma G - 1) + \frac{\rho_e}{\rho_w}\frac{\gamma}{\beta}\frac{dG}{ds}\right) \\ &+ \frac{\gamma}{\beta}\frac{\rho_e}{\rho_w}\left(\frac{dh_m}{ds} - \frac{df_m'}{ds}\right)(1 - 2\gamma G)\left.\right][1 - \gamma G(1 - \gamma/\kappa)]^{-1} \\ = &\, 1 + \frac{1}{m} \end{aligned} \tag{25}$$

where

$$G = \int_0^\infty f'^2 \, d\eta$$

It is necessary to incorporate a Mach-number scaling effect into the coordinates in order to determine the conditions for compressible equilibrium flow. The following transformation allows for this effect:

$$\hat{s} = \int_0^s \frac{\rho_w}{\rho_e} ds, \qquad \hat{\eta} = \left(\frac{\rho_w}{\rho_e}\right)^{1/2} \eta \tag{26}$$

Applying the above transformation, the first integral of the governing equation for arbitrary $\hat{\eta}$ is

$$\begin{aligned} (1 - \hat{\gamma} f')\frac{\partial f}{\partial \hat{s}} = &\, \omega\left(\frac{\rho}{\rho_e}\right)^2 K f'' \\ &- \beta\left(1 + \frac{1}{m} - M_e^2\right)\left[\hat{\eta} f' - \frac{(1 - \hat{\gamma} f')f}{(1 + \gamma/\kappa)}\right] \\ &- \frac{\left(\frac{\gamma}{\kappa}\right)}{(1+\gamma/\kappa)}\beta(1 - \hat{\gamma} f')f\left(M_e^2 - \frac{u_e \dot{v}_w}{\dot{u}_e v_w}\right) + 2\beta\frac{\rho_e}{\rho_w} f - 1 \\ &+ \frac{\hat{\gamma}}{(1+\gamma/\kappa)}\left[\beta\left(1 + \frac{1}{m} - M_e^2 + \frac{\rho_e}{\rho_w}\right)\left(1 - \frac{\gamma}{\kappa}\right)\right. \\ &\left. - 2\frac{\gamma}{\kappa}\beta\left(M_e^2 - \frac{u_e \dot{v}_w}{\dot{u}_e v_w} - \frac{\rho_e}{\rho_w}\right) + 2\gamma\left(\frac{dh_m}{d\hat{s}} - \left(\frac{\rho_w}{\rho_e}\right)^{1/2}\frac{df_m'}{d\hat{s}}\right)\right] \\ &\times \int_0^{\hat{\eta}} f'^2 \, d\hat{\eta} - \frac{\rho_e}{\rho_w}\frac{\beta}{r}\left(1 - \frac{\rho_w}{\rho_e}\right)\left(1 - (1 - r)\frac{\rho_w}{\rho_e}\right) \\ &\times \left[\hat{\eta} f' + \hat{\gamma}\int_0^{\hat{\eta}} f'^2 \, d\hat{\eta}\right] - \hat{\gamma}\frac{\partial}{\partial \hat{s}}\int_0^{\hat{\eta}} f'^2 \, d\hat{\eta} \\ &+ \frac{\gamma}{\left(1 + \frac{\gamma}{\kappa}\right)}\left(\frac{dh_m}{d\hat{s}} - \left(\frac{\rho_w}{\rho_e}\right)^{1/2}\frac{df_m'}{d\hat{s}}\right)(1 - \hat{\gamma} f')f \end{aligned} \tag{27}$$

where

$$\hat{\gamma} = \left(\frac{\rho_w}{\rho_e}\right)^{1/2} \gamma$$

and where the prime denotes partial differentiation with respect to $\hat{\eta}$. Expressions for ω and the density ratio (ρ_e/ρ) can also be written in defect stream-function form:

$$\begin{aligned} \omega = \frac{\delta_i^*}{\delta_v^*} = &\, 1 + 2\gamma\left(\frac{\rho_w}{\rho_e}\right)^{1/2}\left(\frac{\rho_e}{\rho_w} - 1\right) \\ &\times \left\{\int_0^\infty f'^2\left[1 + \frac{\gamma}{2}\left(\frac{\rho_w}{\rho_e}\right)^{1/2} f'\right] d\hat{\eta}\right\} \end{aligned} \tag{28}$$

$$\begin{aligned} \frac{\rho_e}{\rho} = &\, 1 + r\frac{(\bar{\gamma} - 1)}{2} M_e^2\left[1 - \left(\frac{u}{u_e}\right)^2\right] = 1 \\ &- 2\gamma\left(\frac{\rho_w}{\rho_e}\right)^{1/2}\left(\frac{\rho_e}{\rho_w} - 1\right) f'\left[1 + \frac{\gamma}{2}\left(\frac{\rho_w}{\rho_e}\right)^{1/2} f'\right] \end{aligned} \tag{29}$$

Note that, to lowest order, both ω and ρ_e/ρ have approximate values of one. The incompressible form of Eq. (27) is the same as that of Ref. 3.

As in the incompressible case discussed in Ref. 3, the nondimensional shear stress velocity ratio γ is a small parameter. As a result, the defect stream function can be expanded in terms of γ as $f = f_0 + \gamma f_1 + \cdots$ and asymptotic forms of Eqs. (25) and (27) can be obtained. For hypersonic flow, these asymptotic forms are not the strict zero order forms because the term γM_e is not a small parameter. The constrained zero-order forms of Eqs. (25) and (27) are

$$1 + \frac{1}{m} = -\left(\frac{1}{\beta} + 2\frac{\rho_e}{\rho_w} - M_e^2\right) \tag{30}$$

$$\frac{\partial f_0}{\partial \hat{s}} = \omega\left(\frac{\rho}{\rho_e}\right)^2 K f_0'' + (1 + 2\hat{\beta})\hat{\eta} f_0' - f_0 - 1 \tag{31}$$

where the pressure-gradient parameter $\hat{\beta}$ is written as

$$\hat{\beta} = \frac{\rho_e}{\rho_w}\beta\left[1 - \frac{\left(1 - \frac{\rho_w}{\rho_e}\right)}{2r}\left(1 - \frac{\rho_w}{\rho_e}\{1 - r\}\right)\right] \tag{32}$$

The equilibrium condition was defined by Mellor and Gibson[4] to occur when the profiles of f, and hence u, depend on the nondimensional normal coordinate and not the streamwise coordinate. These authors noted that the streamwise partial derivatives are zero when the coefficients of the governing equations are independent of the streamwise coordinate, and they showed that this condition can be met exactly for the zero-order incompressible equation and approximately when higher-order terms are included. This same situation pertains for compressible flow. If K does not depend on $\hat{s}$, $\hat{\beta}$ is constant, and both ω and ρ_e/ρ are approximately one, the coefficients of Eq. (31) are independent of $\hat{s}$ and, since the

boundary conditions are also independent of $\hat{s}$, the derivative on the left side of Eq. (31) is zero. The more complicated coefficients of Eq. (27) depend weakly on $\hat{s}$.

Inner Region Treatment

It is this treatment which most distinguishes the present method of solution from previous methods. In effect, the treatment replaces the surface boundary condition with a condition at the boundary between the inner and outer regions of the boundary layer. The inner region is defined as the part of the boundary layer where the law of the wall and wake pertain. The outer region is defined as the part of the boundary layer where the outer eddy viscosity model pertains. In general, there is one point where both the law of the wall and wake and the outer eddy viscosity model are correct. The present treatment assures that the derivatives of the defect stream function through f'' are continuous at this point.

The inner and outer solutions are not being matched in the formal sense. Actually, these solutions are being patched at one point. As discussed in Ref. 2, this procedure is completely analogous to patching the inner and outer eddy viscosity models in zero-equation models. The inclusion of the wake function in the inner-layer model means that patching can occur beyond the logarithmic part of the boundary layer.

Equation Relating f and f'

An equation can be established which relates f and f' throughout the inner part of the boundary layer. This equation follows from the definition of f and the law of the wall and wake:

$$f = \int_0^{\eta} f' \, d\eta = \eta f' - \int_0^{\bar{\eta}} \eta \left(\frac{\partial g}{\partial \bar{\eta}} + \frac{\partial h}{\partial \bar{\eta}} \right) d\bar{\eta}$$

A relationship between η and $\bar{\eta}$ is needed to form the final inner-region relationship between f and f'. Such a relationship is

$$\frac{\eta}{\bar{\eta}} = \frac{\rho_w}{\rho_e} \left\{ 1 + \frac{1}{\cos^2\theta} \left[\sin^2\theta - 2\chi \left(\tan\theta - \frac{3\chi}{\cos^2\theta} + 2\chi \right) \right] + O\left[\left(\frac{u^*}{a_{aw}} \right)^4 \right] \right\} \tag{33}$$

where θ and χ are defined in Eq. (12). The lowest-order approximate relationship between f and f' is written as

$$f = \eta \left(\frac{\partial f}{\partial \eta} - \frac{1}{\kappa} \right) - \int_0^{\bar{\eta}} \eta \frac{\partial h}{\partial \bar{\eta}} \, d\bar{\eta} + O\left[\left(\frac{u^*}{a_{aw}} \right)^2 \right] \tag{34}$$

Equation (34) pertains throughout the inner region, where the empirical law of the wall and wake is valid. The use of this equation for patching insures the continuity of f and f'. The patch point is positioned so that the derivative f'' is continuous. The transformation given in Eq. (26) is easily applied to the equations of this section.

Patch-Point Location

This location is determined with the equilibrium form of Eq. (27), the first integral of the tangential momentum equation, and Eqs. (9) and (12) for the law of the wall and wake, which are used to evaluate the f'' term in Eq. (27). Equation (34) is used to relate f and f'. With some manipulation, the constrained zero-order governing equation at the patch point is

$$K\omega \frac{\rho_m}{\rho_w} \left\{ \frac{1}{\kappa \bar{\eta}_m} + \left(\frac{\partial h}{\partial \bar{\eta}} \right)_m \right\} + (1 + 2\hat{\beta}) \hat{\eta}_m \left(\frac{\partial f}{\partial \hat{\eta}} \right)_m - f_m - 1 = 0 \tag{35}$$

Using the transformation given in Eqs. (26) and (33), the lowest-order relation between $\hat{\eta}$ and $\bar{\eta}$ is

$$\hat{\eta} = \bar{\eta} \left(\frac{\rho_w}{\rho_e} \right)^{3/2}$$

Because the wake function in Eq. (13) is of order $\bar{\eta}^2$ near the wall, the integral term in Eq. (34) is of order $\bar{\eta}^3$ and can be neglected. If Eq. (34) is substituted into Eq. (35), the equation for the patch-point location, to lowest order, is

$$A\bar{\eta}_m^2 - \bar{\eta}_m + \frac{K}{\kappa} \omega \frac{\rho_m}{\rho_w} = 0 \tag{36}$$

where

$$A = \left(\frac{\rho_w}{\rho_e} \right)^{3/2} \left\{ \frac{1}{\kappa} \left(\frac{\rho_e}{\rho_w} \right)^{1/2} + 2\hat{\beta} \left(\frac{\partial f}{\partial \hat{\eta}} \right)_m \right\} + \frac{12 w_1}{\kappa} K\omega \frac{\rho_m}{\rho_w}$$

Equilibrium Boundary-Layer Solution

A one-parameter shooting technique can be used. The parameter is f'_m, and the condition to be satisfied is the far-field boundary condition, Eq. (23). A value for f'_m is guessed, and Eq. (36) is solved for $\bar{\eta}_m$, which is expressed in terms of the $\hat{\eta}$ coordinate. A value for f_m is obtained from Eq. (34), and the nondimensional shear-stress velocity ratio is evaluated with the equation

$$\gamma = \left[g(\bar{\eta}_m) + h(\bar{\eta}_m) - \left(\frac{\rho_w}{\rho_e} \right)^{1/2} f'(\hat{\eta}_m) \right]^{-1}$$

The equilibrium form of Eq. (27) or (31) is integrated across the boundary layer, and the value of f_∞ is compared with -1. The value of f'_m is iterated until the value of f_∞ converges to -1.

Results and Discussion

Solutions for compressible equilibrium boundary layers have been computed with the constrained zero-order and second-order forms of the present method. As discussed earlier, the constrained zero-order form is not the strict asymptotic form taken in the limit of vanishing nondimensional shear-stress velocity ratio γ, as the term γM_e is not always a small parameter and remains in the formulation. The law of the wall constants κ and B are given the values 0.41 and 4.9, respectively; and the outer-region eddy viscosity constant k is given the value 0.016.

Both constrained zero-order and second-order solutions have been computed over M_e, $\hat{\beta}$, and Re_{δ^*} ranges. The solutions shown were computed with 32 grid points in order to facilitate the wake-function curve fit procedure although significantly fewer points were needed when an analytic wake function was used.

Figure 1 compares velocity defect profiles for the two formulations over a Mach number range for $Re_{\delta^*} = 1 \times 10^4$ and $\hat{\beta} = 0$. It can be seen that the agreement between the formulations is extremely good. Table 1 shows the shear-stress velocity ratio computations to be in agreement within approximately 1%. The difference in γ grows as the edge Mach number decreases. Comparisons over the Reynolds-number range given in Table 1 show that, again, the velocity defect profiles are nearly identical, and the shear-stress velocity ratios differ by approximately 1%. As the Reynolds number decreases, the difference in γ increases. Figure 2 shows the comparison for several $\hat{\beta}$ values for $M_e = 3$ and $Re_{\delta^*} = 1 \times 10^4$. The $\hat{\beta} = 1$ case represents a relatively strong adverse pressure-gradient case for supersonic flow. The velocity-defect agreement for the $\hat{\beta} = 1$ case, although not as good as for the flat plate, is still quite good. The major difference for the $\hat{\beta} = 1$ case occurs in the γ computation where the two solutions differ by just less than 3%. The difference in γ increases with increasingly strong adverse pressure gradient.

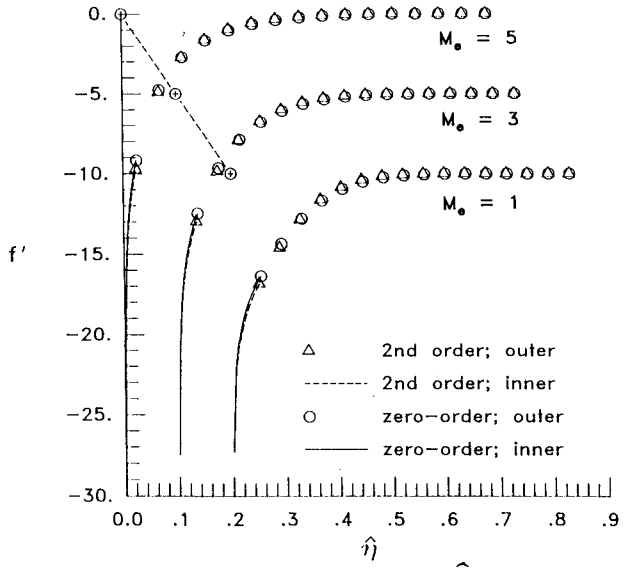

Fig. 1 Effect of M_e on velocity defect profiles ($\hat{\beta} = 0$, $Re_{\delta^*} = 10^4$).

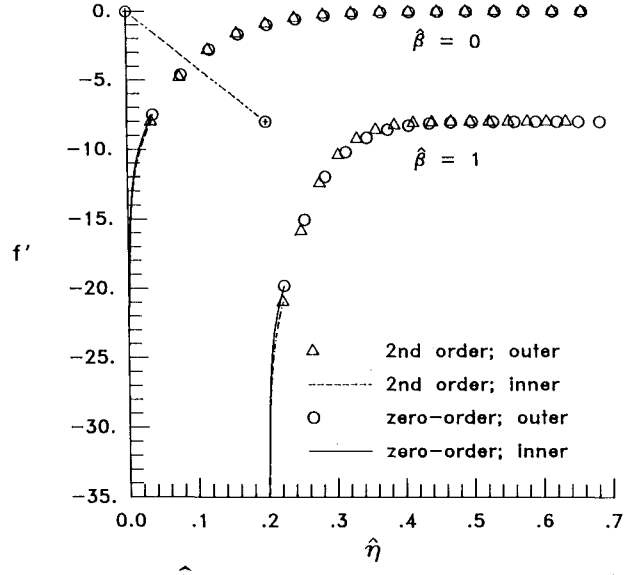

Fig. 2 Effect of $\hat{\beta}$ on velocity-defect profiles ($M_e = 3$, $Re_{\delta^*} = 10^4$).

The reduced complexity of the constrained zero-order formulation and the good agreement of the results discussed above justify it as an excellent approximation and alternative to the second-order formulation. All subsequent solutions shown are based on the constrained zero-order formulation.

The determination of the wake-function coefficient is an important part of the present formulation. The assumed functional form of the wake function was shown in Eq. (13), where w_1 is the coefficient determined by a least-squares curve fit during each iteration of f'_m. Figure 3 compares the resulting analytic wake function to the numerical wake function determined from the difference between the outer velocity defect profile and the assumed law of the wall. These profiles are for $Re_{\delta^*} = 1 \times 10^4$ and $\hat{\beta} = 0$. A standard least-squares correlation factor is used to judge the accuracy of the curve fit. The number of points used for the curve fit varied from case to case in order to maintain approximately the same correlation factor. From Fig. 3, as well as other solutions, it appears that the y^2 dominance of the wake function in the inner region begins to diminish as M_e approaches 4. It can be seen in Fig. 3 that the wake-function coefficient w_1 is a function of M_e in addition to being dependent on $\hat{\beta}$. It was found that w_1 is not a strong function of Re_{δ^*}.

Table 1 Shear-stress velocity ratio comparisons

M_e	$\hat{\beta}$	Re_{δ^*}	$\gamma_{\text{2nd-order}}$	$\gamma_{\text{zero-order}}$
3	0	10^4	0.0409	0.0414
3	0	10^5	0.0341	0.0344
3	0	10^7	0.0256	0.0258
3	1	10^4	0.0367	0.0378
1	0	10^4	0.0375	0.0380
5	0	10^4	0.0435	0.0439

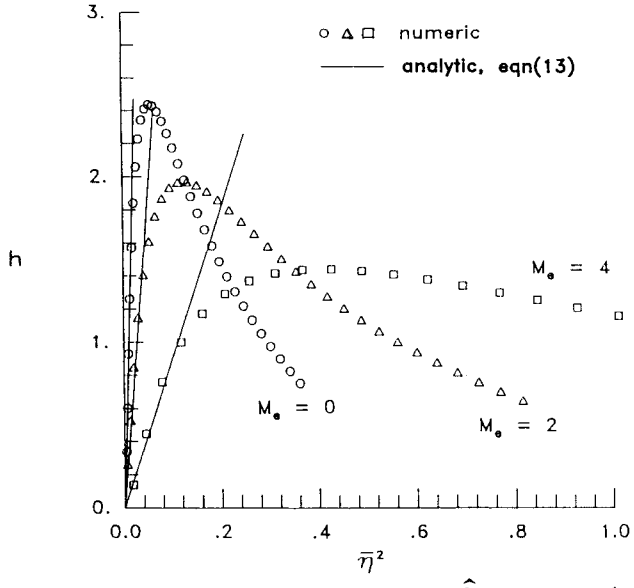

Fig. 3 Analytic and numerical wake functions ($\hat{\beta} = 0$, $Re_{\delta^*} = 10^4$).

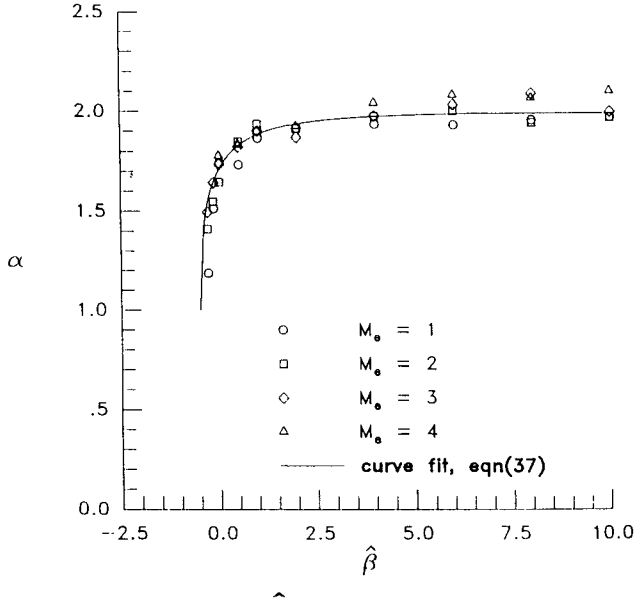

Fig. 4 Effect of $\hat{\beta}$ on wake-function exponent.

An analytic model for the compressible wake-function coefficient based on the above solutions can be written as

$$w_1(M_e,\hat{\beta}) = w_1(0,\hat{\beta})(\rho_w/\rho_e)^{\alpha(\hat{\beta})}$$

where $w_1(0,\hat{\beta})$ is the incompressible wake-function coefficient and the exponent α is a function of $\hat{\beta}$ only. The equation for α was determined from the solutions shown in Fig. 4 to be

$$\alpha(\hat{\beta}) = 2 - \exp\left[-\frac{5}{4}(2\hat{\beta}+1)^{1/2}\right] \qquad (37)$$

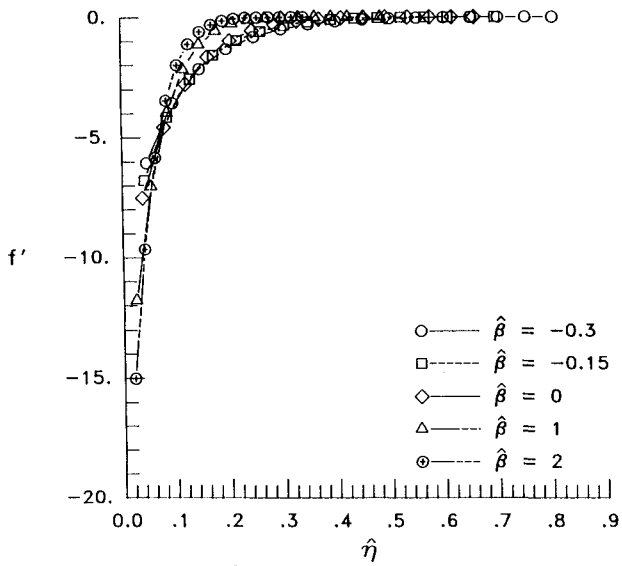

Fig. 5 Effect of $\hat{\beta}$ on zero-order velocity-defect profiles ($M_e = 3$, $Re_{\delta^*} = 10^4$).

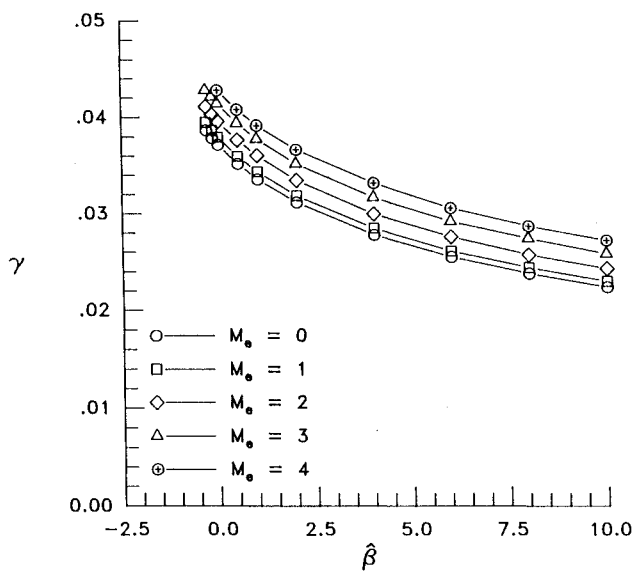

Fig. 6 Effect of $\hat{\beta}$ on shear-stress velocity ratio ($Re_{\delta^*} = 10^4$).

The resulting curve is shown in the figure. The numerical results for incompressible flow are within 10% of the empirical correlation of White; this is comparable to the scatter in the data used in the correlation.

Figure 5 presents a series of constrained zero-order solutions over a $\hat{\beta}$ range from -0.3 to 2 for $Re_{\delta^*} = 1 \times 10^4$ and $M_e = 3$. Since it is unnecessary to evaluate the inner-region solution in order to compute the outer-region solution, only the outer-region results are shown. Results not shown reveal that Mach-number variations have a much smaller effect on the velocity-defect profiles and that Reynolds-number variations have virtually no effect. Figure 6 shows the effect of M_e and $\hat{\beta}$ on the shear-stress velocity ratio for $Re_{\delta^*} = 1 \times 10^4$. It is observed that γ increases with increasing M_e while decreasing with increasing $\hat{\beta}$ (increasingly strong adverse pressure gradient). For any combination of M_e and $\hat{\beta}$, γ increases as the Reynolds number decreases. This trend was documented in Ref. 4 as well as observed in the present investigation.

Comparisons of the constrained zero-order solutions with experimental data from Ref. 12 have also been made. Figure 7 shows the profile comparisons for two flat-plate cases, and

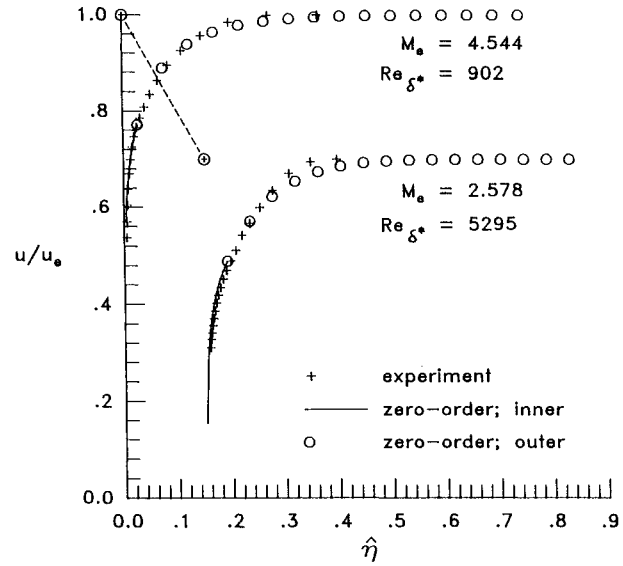

Fig. 7 Comparison of velocity prediction with experiment ($\hat{\beta} = 0$).

Table 2 Shear-stress velocity ratio comparison for compressible flat-plate flow

M_e	Re_{δ^*}	γ_{expt}	γ_{num}	% Difference
1.724	4719	0.0414	0.0420	1.439
2.578	5295	0.0426	0.0431	1.167
4.544	902	0.0544	0.0555	2.002

Table 2 compares the corresponding shear-stress velocity ratios and includes a third flat-plate case. The profile designations from Ref. 12 for the $M_e = 4.544$, $M_e = 2.578$, and $M_e = 1.724$ cases are 53011302, 53010601, and 55010101, respectively. Each case was computed with 32 grid points and the curve-fit procedure for the wake function. The use of the Crocco relation for the density ratio magnifies the velocity differences, especially near the edge of the boundary layer. The modification of the outer eddy viscosity model by including the intermittency factor would improve the comparisons because the gradient of f' would increase as the boundary-layer edge is approached. Table 2 shows excellent agreement between the computed and experimental shear-stress velocity ratios, with differences being less than approximately 2%. The experimental values for γ are based on the values of the skin friction measured with a force balance.

Concluding Remarks

A compressible defect stream-function method has been developed which solves the two-dimensional, turbulent boundary-layer problem. The modified Crocco temperature-velocity relationship is used as an approximation to the energy equation. The difficulty encountered with previous defect stream-function formulations in enforcing the no-slip surface boundary condition is overcome with a law-of-the-wall/law-of-the-wake formulation for the inner part of the boundary layer which is mathematically patched to the outer formulation. This inner formulation eliminates the need for an inner-region eddy viscosity model.

A method for determining the compressible wake function has been developed which involves no additional empirical parameters. An iterative procedure is used to determine the coefficient of the wake function, which is assumed to have a y^2 functional form. Solutions generated with this procedure have been correlated to obtain an analytic compressible wake function.

References

[1]Coles, D., "The Law of the Wake in the Turbulent Boundary Layer," *Journal of Fluid Mechanics*, Vol. 1, Pt. 2, July 1956, pp. 191–226.

[2]Wahls, R. A., Barnwell, R. W., and DeJarnette, F. R., "A Finite-Difference Outer-Layer and Integral Inner-Layer Method for the Solution of the Turbulent Boundary Layer Equations," *AIAA Journal*, Vol. 27, Jan. 1989, pp. 15–22.

[3]Barnwell, R. W., Wahls, R. A., and DeJarnette, F. R., "A Defect Stream Function, Law of the Wall/Wake Method for Turbulent Boundary Layers," *AIAA Journal*, Vol. 27, Dec. 1989, pp. 1707–1713.

[4]Mellor, G. L., and Gibson, D. M., "Equilibrium Turbulent Boundary Layers," *Journal of Fluid Mechanics*, Vol. 24, Pt. 2, Feb. 1966, pp. 225–253.

[5]Clauser, F. H., "The Turbulent Boundary Layer," *Advances in Applied Mechanics*, Vol. 4, Academic Press, New York, 1956, pp. 1–51.

[6]van Driest, E. R., "Turbulent Boundary Layer in a Compressible Fluid," *Journal of the Aeronautical Sciences*, Vol. 18, March 1951, pp. 145–160, 216.

[7]Mager, A., "Transformation of the Compressible Turbulent Boundary Layer," *Journal of the Aeronautical Sciences*, Vol. 25, May 1958, pp. 305–311.

[8]White, F. M., *Viscous Fluid Flow*, McGraw-Hill, New York, 1974, p. 481, 523.

[9]Viegas, J. R., Rubesin, M. W., and Horstmann, C. C., "On the Use of Wall Functions for Two-Dimensional Separated Flows," AIAA Paper 85-0180, Jan. 1985.

[10]Walker, J. D. A., Ece, M. C., and Werle, M. J., "An Embedded-Function Approach for Turbulent Flow Prediction," AIAA Paper 87-1464, June 1987.

[11]Wilcox, D. C., "A Complete Model of Turbulence Revisited," AIAA Paper 84-1076, Jan. 1984.

[12]Fernholz, H. H., and Finley, P. J., "A Critical Compilation of Compressible Turbulent Boundary-Layer Data," AGARDograph No. 223, June 1977.